IEEE Access
Multidisciplinary | Rapid Review | Open Access Journal

SPECIAL SECTION ON TRENDS, PERSPECTIVES AND PROSPECTS OF MACHINE LEARNING APPLIED TO BIOMEDICAL SYSTEMS IN INTERNET OF MEDICAL THINGS

Received August 24, 2018, accepted September 16, 2018, date of publication October 15, 2018, date of current version October 31, 2018.

Digital Object Identifier 10.1109/ACCESS.2018.2873415

Fundus Images-Based Detection and Grading of Macular Edema Using Robust Macula Localization

ADEEL M. SYED[1], M. USMAN AKRAM[2], TAHIR AKRAM[3], MUHAMMAD MUZAMMAL[1,4], SHEHZAD KHALID[1,5], AND MUAZZAM AHMED KHAN[2,6], (Senior Member, IEEE)

[1]Department of Software Engineering, Bahria University, Islamabad 44000, Pakistan
[2]Department of Computer and Software Engineering, National University of Science and Technology, Islamabad 44000, Pakistan
[3]Department of Computer Science, Center of Advanced Studies in Engineering, Islamabad 44000, Pakistan
[4]Department of Computer Science, Bahria University, Islamabad 44000, Pakistan
[5]Department of Computer Engineering, Bahria University, Islamabad 44000, Pakistan
[6]Department of Computing, National University of Science and Technology, Islamabad 44000, Pakistan

Corresponding author: Adeel M. Syed (adeelmuzaffar@gmail.com)

This research is support by IGNITE National Technology Fund, Islamabad, Pakistan, with Grant No. ICTRDF/TR&D/2015/08.

ABSTRACT The macula is an oval-shaped area near the center of the human retina, and at its center, there is a small pit known as the fovea. The fovea contains large concentrations of cone cells and is responsible for sharp, colored vision. Macular disorders are the group of diseases that damage the macula, resulting in blurred vision or even blindness. Macular edema (ME), one of the most common types of macular disorder, is caused by fluid accumulation beneath the macula. In this paper, we present an automated system for the detection of ME from fundus images. We introduce a new automated system for the detailed grading of the severity of disease using knowledge of exudates and maculae. A new set of features is used along with a minimum distance classifier for accurate localization of the fovea, which is important for the grading of ME. The proposed system uses different hybrid features and support vector machines for segmentation of exudates. The detailed grading of ME—as both clinically significant ME and non-clinically significant ME—is done using localized foveae and segmented exudates. The proposed algorithm is validated using public and local data sets. We have achieved an average accuracy of 96.1% in the detection and grading of ME with our proposed method.

INDEX TERMS Biomedical image processing, image analysis, fundus, exudates, macula.

I. INTRODUCTION

Macular edema is the swelling of either the macula or the Müller cells of the retina. The macula is the most sensitive part of the eye and responsible for sharp vision. In macular edema, the patient experiences edema in the macula due to fluid accumulation underneath the macula. This causes the macula to swell and thicken. The macula has very densely-packed cones that are responsible for the minute details in vision. When the macula is swollen, these cones cannot function properly, thus preventing the patient from seeing properly and performing such tasks as driving, reading, or using computers [1].

The causes of macular edema may vary and can be overlapping and interrelated in some cases. Some of the causes include diabetes, aging, cataract surgery, chronic uveitis, blockage of a vein, drug side effects, congenital diseases, etc. [1].

The main symptom of macular edema is blurred vision. When a patient experiences ME, the central part of the vision becomes blurry while the peripheral vision is unaffected. This can lead to obvious problems for the patient since the center part of the vision is needed for almost all essential tasks like reading, driving, or using computers [2].

Macular edema can be classified as either cystoid macular edema or diabetic macular edema [2]. In cystoid macular edema, the blood-retinal barrier in the eye is affected due to any number of reasons, and this leads to the thickening of the retina. As a result, the perifoveal veins in the retina start leaking and fluid begins to accumulate. The accumulation starts in the intracellular spaces of the retina and disrupts the arrangement of the photoreceptors located there. This process is irreversible and is considered to be one of the leading causes of blindness. Diabetic macular edema is caused by the leakage of fluids through the capillaries in the macula [2]. These leaking fluids appear as yellow spots in fundus images known as exudates [2]. It is claimed that there has been an 89% increase in people over 40 years of age suffering from diabetic retinopathy (DR) [1]. This makes DR the foremost cause of blindness in America, affecting approximately 25.8 million people [1]. Clinically Significant

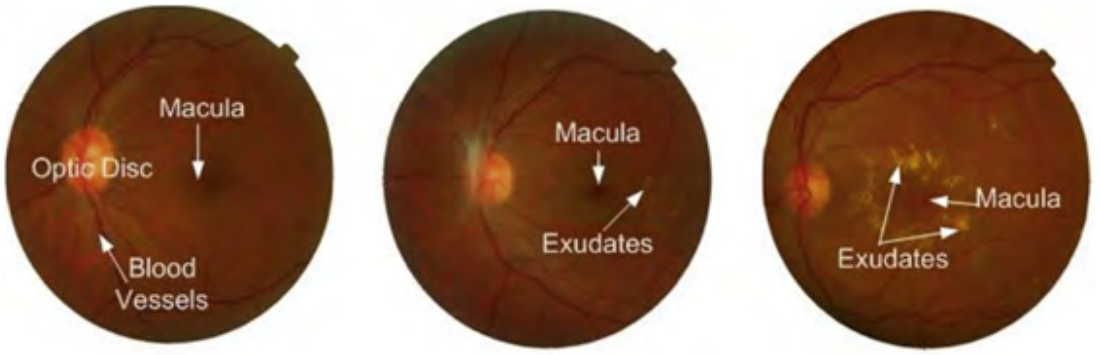

FIGURE 1. Fundus Image showing different stages of macular edema.

Macular Edema (CSME) is one of the main reasons for blindness among patients suffering from diabetes. This accounts for almost 75% of vision loss cases reported [2]. ME is graded as CSME or non CSME based on the existence of exudates in fundus. If exudates appear near or on the macular region, then the condition is graded as CSME; otherwise, it is graded as non CSME [2]. Figure 1 shows fundus images of normal, non CSME, and CSME cases.

This paper consists of 5 sections. Section 2 presents related work in the area of ME. The detailed proposed methodology is explained in Section 3, followed by the results in Section 4. Section 5 describes our conclusions and discussion.

II. LITERATURE REVIEW

A number of researchers have worked on automated analysis of fundus images for the detection of macular edema. Agurto *et al.* [3] used two different databases of 652 and 400 images for detection of exudates and reported their results in terms of AUC. The team claimed to achieve a reading of 0.96 when the combination of both databases was tested against their approach, and a reading of 0.97 when the databases were tested independently. Johny and Thomas [4] checked 30 images for signs of macular edema and determined the severity level of the disease where detected. Of the 30 images checked, their algorithm detected 9 subjects as normal, 8 as moderate, and 13 as severe.

Rekhi *et al.* [5] worked on an algorithm for automatic classification of hard exudates using colored fundus images. They first used adaptive thresholding and then support vector machines (SVM) for classification. They claim to have achieved high accuracy and specificity, with no false positives. The algorithm was tested on 189 images from DIARETDB1 and MESSIDOR. On DIARETDB1, the algorithm achieved an accuracy of 92.13%, and on MESSIDOR, the algorithm achieved an accuracy of 90%.

Rekhi *et al.* [6] created a second algorithm for automated detection and grading of diabetic macular edema from digital color fundus images. The algorithm was tested on 89 images of DIARETDB1 and 100 images of MESSIDOR. In DIARETDB1, the algorithm achieved accuracies of 95.45%, 92.11%, and 87.50% for normal, severe DME, and moderate DME, respectively. On MESSIDOR, accuracies of 92.72%, 90%, and 88.89% were reported for normal, severe DME, and moderate DME, respectively. The researchers claim that the algorithm can be used to determine the severity of the disease.

Acharya *et al.* [7] developed an automated grading algorithm for diabetic macular edema using discrete wavelet transform, discrete cosine transform, and maculopathy index. They claim that the reason for diabetic macular edema is chronic diabetes. Acharaya et al. claimed to achieve an accuracy of 97.01% using publicly available MESSIDOR datasets.

Sengar *et al.* [8] tested 100 fundus images for detection of macular edema using a region-based approach. The images used were from the MESSIDOR database. They achieved an accuracy rate of 80%–90% for different cases. In their paper, they associate the severity of macular edema with the presence of hard exudates in the macular section.

Kunwar *et al.* [9] researched the detection of high-risk macular edema. They did this with the help of texture features and an SVM classifier. They claim to have achieved an accuracy of greater than 86%. Sensitivity achieved was 91%, and specificity was 75%.

Kumar and Ravichandran [10] performed a severity test in the detection of macular edema using colored fundus images. They conducted their research using an extreme learning machine classifier and common features like texture, color, and intensity. The algorithm had 99.0% sensitivity and specificity ranging between 85.0% and 98.0%.

Many applications use automated means for collecting healthcare data [11]—for example, using automated body sensor networks for tasks such as heart rate monitoring [12], life cycle management [13], and others [14].

The methods presented in literature mostly focus on binary-level detection, meaning they detect whether a fundus image is ME or not based on the existence of exudates. Very rarely is work is done on detailed grading of ME, and it generally utilizes small local datasets. There is no publicly available fundus image dataset that provides annotations for

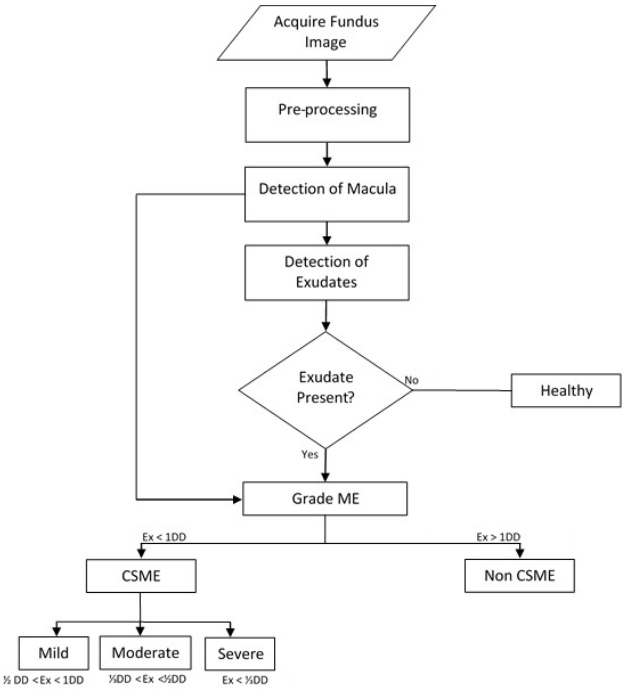

FIGURE 2. Flow Diagram of the system. Here Ex stands for Exudates and DD stands for one-disc diameter.

detailed grading. In this paper, we propose a new fundus image analysis method which provides detailed automated grading of ME. This paper contributes to the existing literature by yielding a precise quadrant-wise severity of ME. Evaluation of our method was done using public and local datasets, and extra annotations were gathered with help of two ophthalmologists.

III. PROPOSED METHODOLOGY

The proposed system presents an automated method for the detection and grading of macular edema (ME). Figure 2 shows a flow diagram of the proposed system with all included subblocks. The main modules are macula detection, segmentation of exudates, and grading of ME. The proposed system further subgrades the severity levels of CSME and provides a detailed quadrant-wise analysis.

A. PREPROCESSING

The first stage of proposed algorithm is preprocessing in which multiple steps are carried out to improve the quality of input image. Preprocessing stage first separates foreground (fundus region) from background so that all upcoming steps only consider fundus region. This is carried out using adaptive thresholding followed by morphological operations [15]. Second step in preprocessing stage is to improve contrast between different components i.e. blood vessels, macula, optic disc etc. and fundus background. We are using histogram equalization, for contrast enhancement. In order to cater noise issues, clip limited adaptive histogram equalization is used.

B. MACULA DETECTION

In this paper, a new supervised training-based method for macula detection is presented. Figure 3 shows the system level diagram of proposed macula detection algorithm. The algorithm takes original fundus images and their corresponding, manually extracted, macular region for generation of a supervised training feature vector. In testing phase, same features for all possible candidate macular regions are extracted and then they are passed to minimum distance classifier. The classifier selects the region with closest distance from training feature vector.

1) GENERATION OF FEATURE SET FOR TRAINING

The main step of training the system is generation of the feature set. In this step, we crop the macular region manually for all training images. The next step is to represent macula regions with the best features. These features are selected so as to represent actual behavior of maculae in fundus images (location, appearance, etc.). The following four features are extracted:

- Area of Macula (f1): It represents total number of pixels a macular region contains.
- Distance from the Optic Disc (f2): This feature computes the distance between optic disc center and macula region center
- Mean Intensity (f3): Macula region is normally blackish in color and in order to differentiate macula region from other dark regions in fundus image like hemorrhages and blood vessel, mean intensity is taken as feature.
- Angle between the Macula and the Optic Disc (f4): Forth feature is angle between optic disc and macula.

All of these features are used to classify the regions in the testing stage. These features are all normalized, and the average of the features is used to determine the normalized mean feature for the macula, which is used later with the minimum distance classifier for testing.

2) AUTOMATIC MACULA DETECTION FOR TEST IMAGE

Following generation of the training feature vector, the second phase of the proposed system is analyzing fundus images for automated detection of macula. This phase extracts all possible macular candidate regions in addition to the features mentioned above to detect actual macula location. This stage first applies adaptive thresholding technique to extract all possible candidate regions which may contain macula (Fig. 4 (b)). The macula region has a similar intensity to that of blood vessels and some lesions such as hemorrhages. This can make macula detection a bit tricky. In the proposed system, we remove vessel pixels from all candidate macula regions to eliminate false candidate regions. Blood vessels are extracted using Gabor wavelets and multilayer thresholding techniques as proposed in [16] (Fig. 4(c)). These extracted blood vessels are removed from candidate regions to eliminate false positives which occur due to similarity between vessels and macula regions (Fig. 4(d)). These regions are then

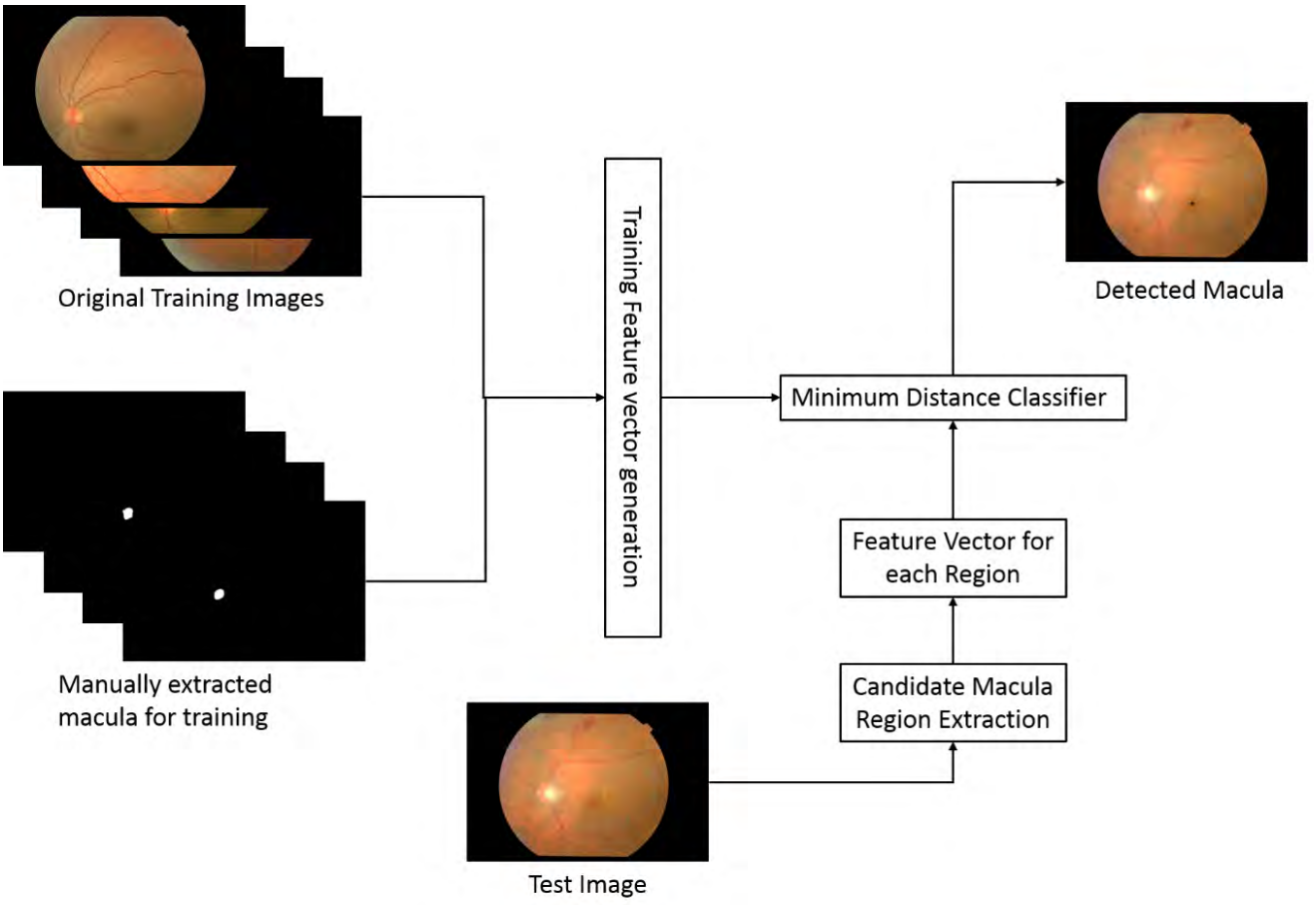

FIGURE 3. System level diagram for proposed macula detection algorithm.

classified as separate regions using connected component labeling (Fig. 4(e)).

Next, each of these regions is considered for classification, and features are extracted for each region. In order to find the distance from the optic disc to both the region (F2) and angle (F4), we need to locate the optic disc (prior knowledge of the optic disc is critical here). For optic disc localization, first all bright regions from the fundus image are extracted using adaptive thresholding. As this may also include exudates or other bright lesions as false regions, blood vessel density in each candidate region is calculated, and the region with maximum blood vessel density is then correctly selected as the optic disc region [17].

3) FEATURE EXTRACTION OF MACULAR REGION

The extraction stage mentioned above calculates area of macula, distance from the optic disc, mean intensity, and angle from the optic disc. All of these features are extracted for each candidate region. Table 1 shows 8 sample regions taken from a single fundus image whose features have been extracted. The first entry in the table is for the true macula region, and it is evident that the extracted features clearly discriminate between true and false macula regions.

TABLE 1. Features extracted from a Fundus Image.

Region No.	Area of Macula	Distance from OD	Mean Intensity	ME
1.	**5.193**	**0.807**	**13.994**	**0.565**
2.	0.002	0.707	0.011	0.745
3.	0.003	0.824	0.018	1.143
4.	0.003	0.919	0.015	1.148
5.	0.009	0.870	0.056	1.273
6.	0.002	0.632	0.011	1.270
7.	0.030	0.616	0.163	0.718
8.	0.002	0.906	0.013	1.552

4) MINIMUM DISTANCE CLASSIFIER

Minimum distance classifier is used in the selection of the macula from all the candidate regions. Mean value from the training set feature vector is calculated and then saved for reference and comparison with other candidate regions. The distance between each candidate region's feature vector and training feature vector is calculated. The region with the minimum distance is selected as the macula. Figure 4 shows the step-by-step output for a macula detection module taken from a randomly selected fundus image.

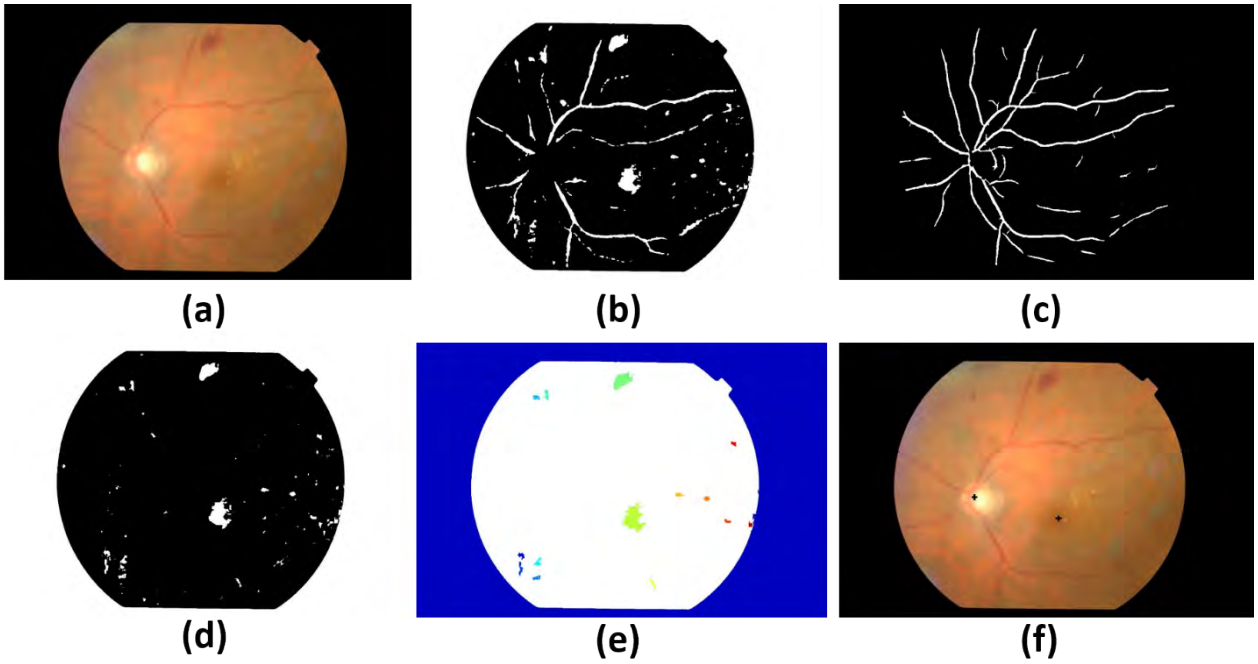

FIGURE 4. Macula detection. (a) input image, (b) adaptive thresholding result for dark regions, (c) blood vessel detection, (d) candidate regions after removal of blood vessels, (e) Labelled candidate regions, (f) Detected macula.

5) EXUDATE DETECTION

In order to automatically grade a macular disease, the most challenging part is accurate identification of lesions in the fundus image. In our case, we are looking for exudates that show up as bright yellow spots on the image. The intensity of regions containing exudates is found to be higher than the neighboring regions. Our approach first finds all the candidate regions that are likely to be exudates. Later, with the help of features and support vector machines, true exudate detection is possible.

6) SEGMENTATION FOR EXUDATE REGION

In this stage of the algorithm, we try to rule out all the candidate exudates or the regions where the exudates are detected. Our algorithm is explained in the following steps:

1. Input preprocessed image
2. Apply morphological closing [using Equation 1] to suppress the dark lesions and blood vessels
3. Apply adaptive contrast enhancement technique [using Equation 2 and Equation 3] to improve contrast of bright lesions
4. Apply Gabor filter [using Equation 4] to further enhance contrast of all the bright lesions
5. Apply OSTU's algorithm to convert the image to binary
6. Remove the optic disc and blood vessels (if present and already not removed)
7. Classify the resulting areas as candidate regions for presence of exudates

$$\emptyset_f^{(SB)} = min[maxf\ (x+b)\,] \tag{1}$$

Here SB is taken as the structuring element.

$$g = 255\frac{\left[\Phi_\omega\left(\emptyset_f\right) - \Phi_\omega\left(\emptyset_{fmin}\right)\right]}{\left[\Phi_\omega\left(\emptyset_{fmax}\right) - \Phi_\omega\left(\emptyset_{fmin}\right)\right]} \tag{2}$$

Here $\emptyset_f$ is calculated by the above equation (Equation 1) while Φ_ω is calculated by the following equation (Equation 3). $\emptyset_{fmin}$ and $\emptyset_{fmax}$ are minimum and maximum intensities. Also, in the following equation, the mean and variance of these intensities are given by m_ω and σ_w.

$$\Phi_\omega\left(\emptyset_f\right) = \left[1 + exp\left(\frac{m_\omega - \emptyset_f}{\sigma_w}\right)\right]^{-1} \tag{3}$$

$$FB_G = \frac{1}{\sqrt{\pi r}\sigma} e^{-\frac{1}{2}\left[\left(\frac{d_1}{\sigma}\right)^2 C\left(\frac{d_2}{\sigma}\right)^2\right]} (d_1 cos\Omega + d_1 sin\Omega) \tag{4}$$

Here 'r' is the aspect ratio while 'σ' represents standard deviation. Spatial frequency is represented by 'Ω'. The orientation of the filter is represented by θ, then the values of d_1 can be calculated by Equation 5.

$$d_1 = xcos\theta + ysin\theta \tag{5}$$

and the values of d_2 can be calculated by Equation 6.

$$d_2 = -xcos\theta + ysin\theta \tag{6}$$

By varying parameters, a number of filters are generated. All filters are convolved with image to generate an enhanced version. The convolution is represented by the following equation (Equation 7).

$$FB_R(s,t) = \sum_x \sum_y I_c(x,y)\, FB_G(s-x, t-y) \tag{7}$$

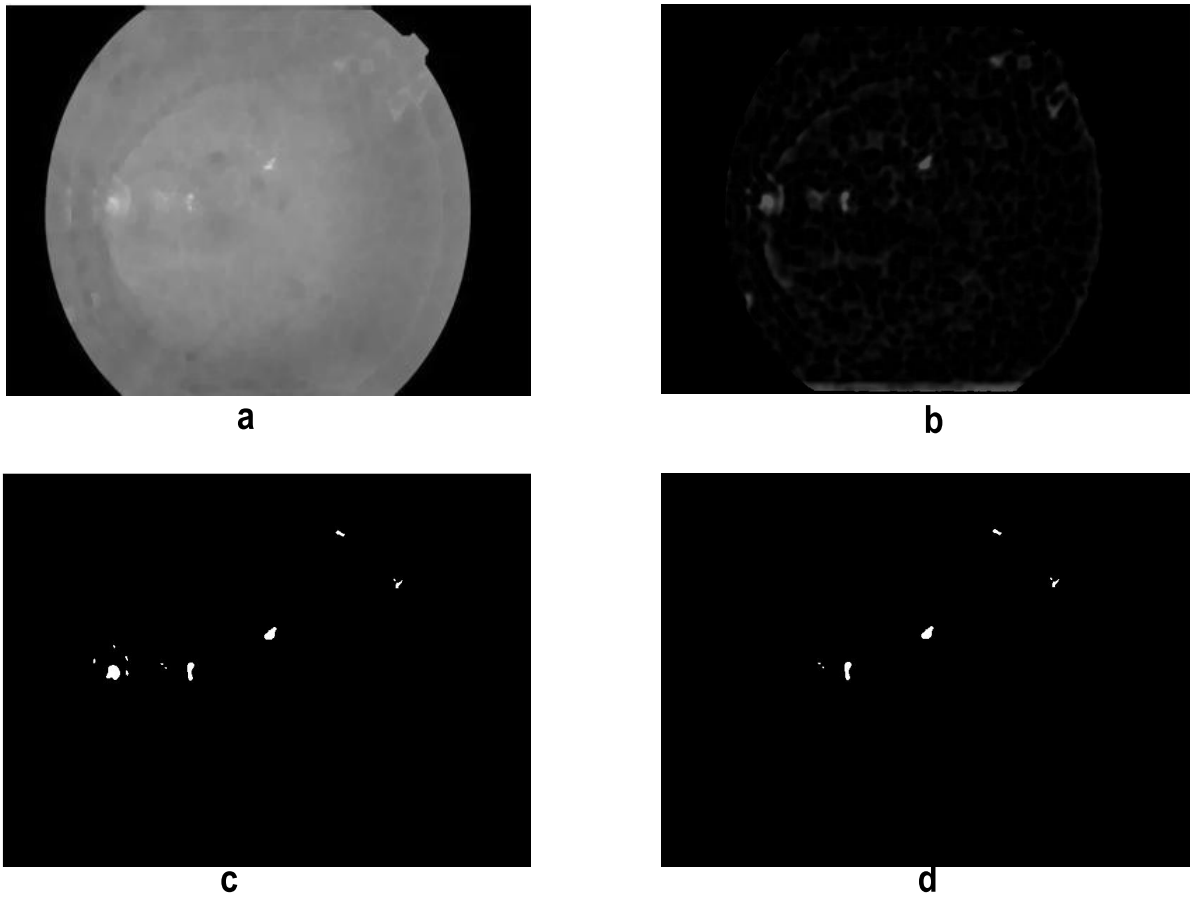

FIGURE 5. (a) Contrast enhanced image (b) Results after applying Gabor filtering (c) Application of OTSU's algorithm (d) Result after removal of OD.

Towards the end of this phase, the image is transformed into a binary image with the help of adaptive thresholding. In addition, the optic disc is detected and removed. The results of this stage are given in Figure 5.

7) FEATURE EXTRACTION FOR EXUDATE REGION

Once the candidate regions are identified, we can then extract the features. The features are calculated for both exudate regions and non-exudate regions. We calculate the following features:

- Feature 1: Green channel, maximum intensity.
- Feature 2: Green channel, minimum intensity.
- Feature 3: Red channel, mean intensity.
- Feature 4: Red channel, maximum intensity.
- Feature 5: Red Channel, minimum intensity.

These features are combined to form a feature vector, which is calculated for each region. Then we proceed to the classification stage, where we determine whether the region is an exudate region or a non-exudate region.

8) CLASSIFICATION

Support vector machines (SVMs) are learning algorithms that are supervised and linked with other learning algorithms. These are generally used for regression analysis and classification.

In SVM, the idea is to find a hyperplane in such a way that the difference between the two classes is the maximum difference possible. Mathematically, the following equation (Equation 8) separates the two classes:

$$y_i (W \cdot X + b) \geq 0 \tag{8}$$

where W is the weight vector having all the weights and b is a scalar value.

There can be many hyperplanes possible, but what we are interested in is the hyperplane with the greatest distance between the planes. This is known as the margin and can be calculated by Equation 9

$$m = \frac{2}{|w|} \tag{9}$$

where m is the margin. So, we are looking for the hyperplane with the greatest margin. The kernel that we have used to train our dataset is the quadratic kernel. The results of the application of SVM classifier is given in Figure 6.

C. GRADING OF MACULAR EDEMA

This is the final stage in the grading of the disease. In this phase, we determine the severity of the disease if present. The grading criteria depend upon the distance between the

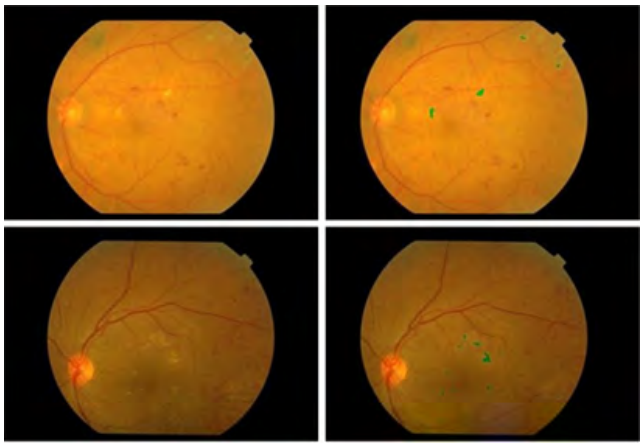

FIGURE 6. Final results of Exudate Detection.

TABLE 2. Benchmark for grading of Macular Edema.

Grade	Condition Detected	Classified as:
0	No exudates detected	Healthy
1	Exudates present and $\|d\| > 1\,DD$	Non CSME
2	Exudates present and $1/2 < \|d\| \leq 1\,DD$	Mild CSME
3	Exudates present and $1/3 < \|d\| \leq 1/2\,DD$	Moderate CSME
4	Exudates present and $\|d\| \leq 1/3\,DD$	Severe CSME

exudate and macula. The clinical standard used for the grading of ME is elaborated in Table 2. If there are no exudates detected, then the fundus image is considered healthy. Otherwise, if exudates are detected, then depending upon the distance of exudates from the macula, we classify them as Non CSME, Mild CSME, Moderate CSME, or Severe CSME. This is a major contribution of our research, as we are now able to automatically grade the presence of ME in a fundus image. This can assist an ophthalmologist in analysis of the disease.

Where Δx represents the distance between the exudates and the location of the macula and DD is the diameter of the optic disc. The distance computed is the Euclidian distance. It is calculated by equation 10 given below:

$$|\boldsymbol{d}| = \sqrt{\boldsymbol{\Delta x^2} + \Delta \boldsymbol{y^2}} \tag{10}$$

where

$$\boldsymbol{\Delta x} = \boldsymbol{x_2} - \boldsymbol{x_1}$$
$$\boldsymbol{\Delta y} = \boldsymbol{y_2} - \boldsymbol{y_1}$$

While grading ME, we further divide the region according to the Inferior Superior Nasal Temporal (ISNT) rule. The ISNT rule is used clinically to identify affected regions. Each region is highlighted with different colors corresponding to the ratio of the affected area to the overall area. Figure 7 shows quadrant-wise severity of effectiveness as well as the ranges for different colors and grades.

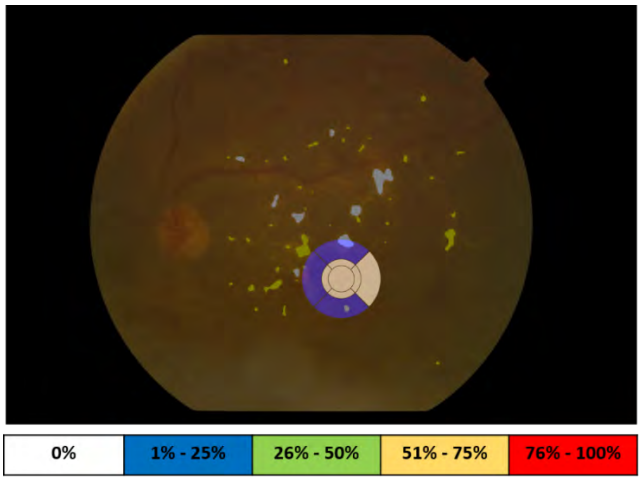

FIGURE 7. Quadarant wise ME grading with color scheme.

TABLE 3. database Description.

Database	Total	Normal	ME	CSME	Non CSME
DRIVE	40	33	7	4	3
DIARETDB1	89	5	84	30	54
MESSIDOR	1200	971	229	154	75
AFIO	462	160	302	187	115
Total	**1791**	**1169**	**622**	**375**	**247**

TABLE 4. Mean Feature vector for macula with standard deviations for different databases.

Database	Area (f1) mean±std	Mean Intensity (f2) mean±std	Distance from OD (f3) mean±std	Angle with OD (f4) mean±std
DRIVE	0.0230±0.0066	0.1648±0.0618	0.4415±0.0559	0.1633±0.1417
DIARETDB	0.0302±0.0170	0.0497±0.0322	0.4351±0.0385	0.0525±0.0449
MESSIDOR	0.0336±0.0166	0.0357±0.0088	0.4239±0.0953	0.1152±0.0521
AFIO	0.0195±0.0076	0.0816±0.0412	0.3202±0.0241	0.1514±0.0726

IV. RESULTS

Evaluation of the proposed system is carried out using multiple public and local datasets. These datasets do not contain annotations for grading; therefore, in order to perform detailed grading for evaluation, each dataset is further annotated with the help of two ophthalmologists. The ophthalmologists classify each image as either CSME or non CSME and then further grade the CSME cases as mild, moderate, or severe. The online datasets used are DRIVE [18], DIARETDBI [19], and MESSIDOR [20]. Table 3 shows a detailed description of all datasets. It clearly highlights the number of both normal and macular edema cases as well as their further division into CSME and non CSME. DRIVE dataset mostly have normal subjects where as DIARETDB1 and AFIO datasets have large number of ME subjects.

TABLE 5. Results of Macula detection.

Database	Total Images	Detected Correctly	Accuracy %
DRIVE	40	40	100
DIARETDB1	89	84	94.38
MESSIDOR	1200	1123	93.50
AFIO	462	439	95.02
Total	**1791**	**1686**	**94.13**

TABLE 6. Comparison of ME detection methods with existing methods.

Method	Sensitivity (%)	Specificity (%)	Database
A. Sopharak et al. [21]	80.00	99.46	Local
OSAREH et al. [22]	96.00	94.60	Local
A.W. Reza et al. [23]	94.90	100	STARE
M. Garcia et al. [24]	100	92.59	Local
Ranamuka, N. G. et al [25]	75.43	99.99	DIARETDB0 DIARETDB1
Jaafat et. al. [26]	98.9	91	DIARETDB0
K. Sai Deepak et. al. [27]	95	90	MIAS MESSIDOR
Our Proposed Method	**96.23±0.13**	**95.04±0.48**	**Average**

TABLE 7. ME Grading Results.

Database	Sensitivity	Specificity	Accuracy
DRIVE	100±0.001	96.96±0.17	97.5±0.19
DIARETDB	96.42±0.29	80±0.51	95.50±0.34
MESSIDOR	97.37±0.63	98.5±0.70	98.33±0.82
AFIO	95.03±0.86	89.3±0.32	93.07±0.84

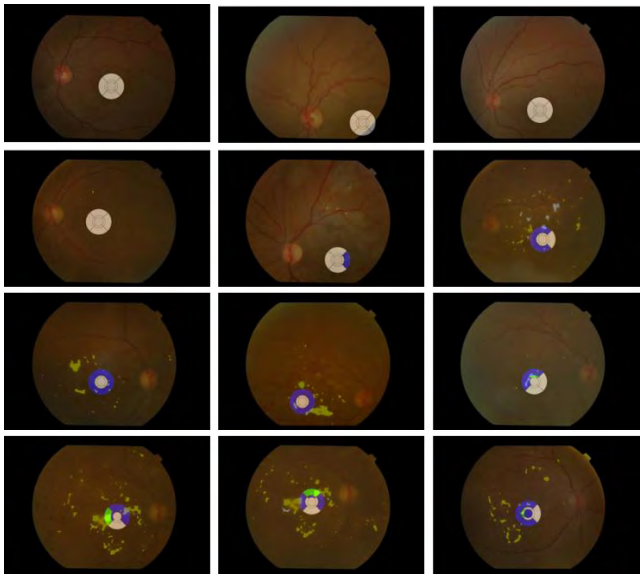

FIGURE 8. Fundus images classified as normal, non CSME, mild, moderate or severe.

While evaluating proposed system, first evaluation is one for macula detection. For macula detection, mean feature vectors are generated for training images from each dataset. Table 4 shows these mean feature vectors. These mean feature vectors are used in minimum distance classifier to classify each candidate region from test image as macular or non macular regions.

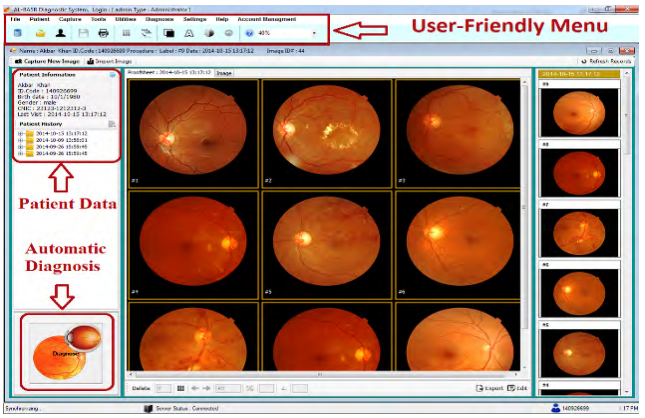

FIGURE 9. GUI of Al BASR System.

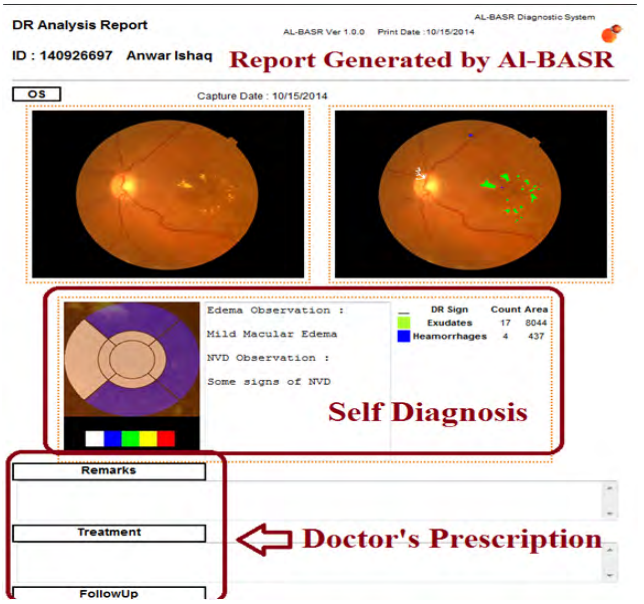

FIGURE 10. Report generated by Al-BASR.

Table 5 shows macula detection module results for different datasets. DRIVE mostly have normal subjects and images are of good quality so proposed system showed 100% results on that. However, in case of other datasets with more ME cases, the accuracy is still above 93%.

In exudate detection and diagnosis of ME, 10-fold cross validation technique is used as it is the most used cross validation scheme for this application. We have compared the proposed technique with existing methods as shown in Table 6. It is clear from table that proposed system outperforms existing methods even for a large dataset.

ME grading results are presented in Table 7. The table presents data from the aforementioned databases (DRIVE, DIARETDB, MESSIDOR and AFIO). Figure 8 shows some random cases where we have shown how different fundus images are classified as Normal, non CSME, mild CSME, moderate CSME, or severe CSME. The first row shows cases where input images are classified as normal. From the second row down and from left to right, the severity level increases

and different examples for non CSME, mild CSME, moderate CSME, and severe CSME are shown. This grading method can be used for real-time assessment of different cases and to help ophthalmologist in screening of patients.

V. CONCLUSION

We have presented an automated method for the detection and grading of macular edema. Our approach detects both the location of exudates and the location of the macula. Following this, depending on the distance between the macula and the exudates, the severity of the disease is classified. The grading is done as explained in Table 2. Therefore, by examining the distance of exudates from the macula, we are able to mark the images as normal, mild, moderate, or severe. Our approach yielded excellent results and was tested on four separate datasets, three of which are publicly available. This proposed approach is embedded in a real-time hospital management system named AL-BASR, which is being used in a local hospital to generate automated reports for each patient undergoing fundus scans (www.albasr.com). Figure 9 shows a screen shot of the AL-BASR system. AL-BASR has the capability to perform automatic diagnoses on fundus images for retinal diseases.

AL-BASR analyzes fundus images and generates a report based on its findings using image processing and machine learning-based algorithms. The research carried out in this thesis is used in Al-BASR for detection and grading of macular edema. Figure 10 shows a report generated through Al-BASR, and all findings are highlighted in the report.

ACKNOWLEDGMENT

The authors are also thankful to AFIO, Rawalpindi, Pakistan for providing them with the dataset to conduct this research.

REFERENCES

[1] *Vision Problems in the U.S.—Prevalence of Age-Related Eye Disease in America*. [Online]. Available: http://www.visionproblemsus.org/index.html
[2] F. K. P. Sutter, M. C. Gillies, and H. Helbig, "Diabetic macular edema: Current treatments," in *Medical Retina*. Berlin, Germany: Springer, 2007, pp. 131–146.
[3] C. Agurto *et al.*, "A multiscale optimization approach to detect exudates in the macula," *IEEE J. Biomed. Health Informat.*, vol. 18, no. 4, pp. 1328–1336, Jul. 2014.
[4] A. Johny and A. Thomas, "A novel approach for detection of diabetic macular edema," in *Proc. Int. Conf. Emerg. Trends Eng., Technol. Sci. (ICETETS)*, Feb. 2016, pp. 1–4.
[5] R. S. Rekhi, A. Issac, M. K. Dutta, and C. M. Travieso, "Automated classification of exudates from digital fundus images," in *Proc. Int. Conf. Workshop Bioinspired Intell. (IWOBI)*, Jul. 2017, pp. 1–6.
[6] R. S. Rekhi, A. Issac, and M. K. Dutta, "Automated detection and grading of diabetic macular edema from digital colour fundus images," in *Proc. 4th IEEE Uttar Pradesh Sect. Int. Conf. Elect., Comput. Electron. (UPCON)*, Oct. 2017, pp. 482–486.
[7] U. R. Acharya *et al.*, "Automated diabetic macular edema (DME) grading system using DWT, DCT features and maculopathy index," *Comput. Biol. Med.*, vol. 84, pp. 59–68, May 2017.
[8] N. Sengar, M. K. Dutta, R. Burget, and L. Povoda, "Detection of diabetic macular edema in retinal images using a region based method," in *Proc. 38th Int. Conf. Telecommun. Signal Process. (TSP)*, Jul. 2015, pp. 412–415.
[9] A. Kunwar, S. Magotra, and M. P. Sarathi, "Detection of high-risk macular edema using texture features and classification using SVM classifier," in *Proc. Int. Conf. Adv. Comput., Commun. Inform. (ICACCI)*, Aug. 2015, pp. 2285–2289.
[10] S. J. J. Kumar and C. G. Ravichandran, "Macular edema severity detection in colour fundus images based on ELM classifier," in *Proc. Int. Conf. I-SMAC (IoT Social, Mobile, Anal. Cloud) (I-SMAC)*, Feb. 2017, pp. 926–933.
[11] W. Wu, H. Zhang, S. Pirbhulal, S. C. Mukhopadhyay, and Y. T. Zhang, "Assessment of biofeedback training for emotion management through wearable textile physiological monitoring system," *IEEE Sensors J.*, vol. 15, no. 12, pp. 7087–7095, Dec. 2015.
[12] S. Pirbhulal, H. Zhang, W. Wu, S. C. Mukhopadhyay, and Y.-T. Zhang, "Heart-beats based biometric random binary sequences generation to secure wireless body sensor networks," *IEEE Trans. Biomed. Eng.*, to be published, doi: 10.1109/TBME.2018.2815155.
[13] A. H. Sodhro, S. Pirbhulal, and A. K. Sangaiah, "Convergence of IoT and product lifecycle management in medical health care," *Future Gener. Comput. Syst.*, vol. 86, pp. 380–391, Sep. 2018, doi: 10.1016/j.future.2018.03.052.
[14] W. Wu, S. Pirbhulal, A. K. Sangaiah, S. C. Mukhopadhyay, and G. Li, "Optimization of signal quality over comfortability of textile electrodes for ECG monitoring in fog computing based medical applications," *Future Gener. Comput. Syst.*, vol. 86, pp. 515–526, Sep. 2018.
[15] U. Akram, "Retinal image preprocessing: Background and noise segmentation," *Indonesian J. Elect. Eng. Comput. Sci.*, vol. 10, no. 3, pp. 537–544, 2012.
[16] M. U. Akram and S. A. Khan, "Multilayered thresholding-based blood vessel segmentation for screening of diabetic retinopathy," *Eng. Comput.*, vol. 29, no. 2, pp. 165–173, 2013.
[17] A. Usman, S. A. Khitran, M. U. Akram, and Y. Nadeem, "A robust algorithm for optic disc segmentation from colored fundus images," in *Proc. Int. Conf. Image Anal. Recognit.* Cham, Switzerland: Springer, 2014, pp. 303–310.
[18] DRIVE. Accessed: Jun. 30, 2018. [Online]. Available: http://www.isi.uu.nl/Research/Databases/DRIVE
[19] *DIARETDB1*. Accessed: Jun. 30, 2018. [Online]. Available: http://www2.it.lut.fi/project/imageret/diaretdb1/
[20] *MESSIDOR*. Accessed: Jun. 30, 2018. [Online]. Available: http://www.adcis.net/en/Download-Third-Party/Messidor.html
[21] A. Sopharak, B. Uyyanonvara, S. Barman, and T. H. Williamson, "Automatic detection of diabetic retinopathy exudates from non-dilated retinal images using mathematical morphology methods," *Comput. Med. Imag. Graph.*, vol. 32, no. 8, pp. 720–727, 2008.
[22] A. Osareh, B. Shadgar, and R. Markham, "A computational-intelligence-based approach for detection of exudates in diabetic retinopathy images," *IEEE Trans. Inf. Technol. Biomed.*, vol. 13, no. 4, pp. 535–545, Jul. 2009.
[23] A. W. Reza and C. Eswaran, "A decision support system for automatic screening of non-proliferative diabetic retinopathy," *J. Med. Syst.*, vol. 35, no. 1, pp. 17–24, 2011.
[24] M. García, C. I. Sánchez, M. I. López, D. Abásolo, and R. Hornero, "Neural network based detection of hard exudates in retinal images," *Comput. Methods Programs Biomed.*, vol. 93, no. 1, pp. 9–19, 2009.
[25] N. G. Ranamuka and R. G. N. Meegama, "Detection of hard exudates from diabetic retinopathy images using fuzzy logic," *IET Image Process.*, vol. 7, no. 2, pp. 121–130, 2013.
[26] H. F. Jaafar, A. K. Nandi, and W. Al-Nuaimy, "Decision support system for the detection and grading of hard exudates from color fundus photographs," *J. Biomed. Opt.*, vol. 16, no. 11, p. 116001, 2011.
[27] K. S. Deepak, N. V. K. Medathati, and J. Sivaswamy, "Detection and discrimination of disease-related abnormalities based on learning normal cases," *Pattern Recognit.*, vol. 45, no. 10, pp. 3707–3716, 2012.

ADEEL M. SYED received the B.S. and M.S. degrees in software engineering from Bahria University Islamabad Campus in 2007 and 2010, respectively, where he is currently pursuing the Ph.D. degree in software engineering. He have submitted the thesis for evaluation for his Ph.D. degree. He is currently a Senior Assistant Professor with the Department of Software Engineering, Bahria University Islamabad. The main research areas are bio medical image analysis and pattern recognition.

M. USMAN AKRAM received the B.S. degree (Hons.) in computer system engineering and the master's and Ph.D. degrees in computer engineering from the College of Electrical and Mechanical Engineering, National University of Sciences and Technology (NUST), Rawalpindi, Pakistan, in 2008, 2010, and 2012, respectively. He is currently an Associate Professor with the College of Electrical and Mechanical Engineering, NUST. His main areas of research are biomedical imaging and image processing. He has over 200 international publications in well-reputed journals and conferences.

TAHIR AKRAM received the B.Sc. degree in telecommunication engineering from the University of Azad Jammu and Kashmir and the M.S. degree in electrical engineering from the University of Engineering and Technology, Taxila. He is currently pursuing the Ph.D. degree in computer science with COMSATS University Islamabad. His research interests are medical image/signal processing, and machine learning.

MUHAMMAD MUZAMMAL received the bachelor's degree from IIU, Pakistan, in 2005, and the master's degree from FAST-NU, Pakistan, in 2005, and the Ph.D. degree from the University of Leicester, U.K., in 2012. He was a Software Analyst at LMKR. He is currently an Associate Professor with the Department of Computer Science, Bahria University, Islamabad, Pakistan, a Visiting Associate Professor under the CAS President's International Fellowship Initiative at the Centre of Big Mobile Intelligence, Shenzhen Institutes of Advance Technology, Chinese Academy of Sciences, Shenzhen, and a Vice Director of the Guangdong Provincial R&D Centre of Blockchain and Distributed IoT Security, Guangdong, China. He is interested in blockchain technology with a focus on decentralized systems and mining. His research interests are in large-scale data mining, including algorithm design and mobility data mining.

SHEHZAD KHALID received the Ph.D. degree from The University of Manchester, U.K., in 2009. He is currently a Professor and the Director of the Research, Bahria University, Pakistan. He is a qualified academician and a researcher with over 125 International publications in reputed journals and international conferences. He has also authored various books and book chapters. His main areas of research include biomedical imaging, computer visions, pattern recognition, natural language processing, sentiment analysis, and time series analysis.

MUAZZAM AHMED KHAN (SM'15) received the Ph.D. degree in computer sciences, as sandwich program, from IIUI and UMKC, USA, in 2011. He is currently the Senior Head of the department at the NUST School of Electrical Engineering and Computer Science. He is also an Assistant Professor with the Department of Computing. His research interests include wireless networks sensor, image processing, and data and network security.